

Synthesis, structure, and ionic conductivity of $\text{Na}_5\text{Li}_3\text{Ti}_2\text{S}_8$

Fu Qiang Huang^a, Jiyong Yao^b, Zhanqiang Liu^a, Jianghua Yang^a, James A. Ibers^{b,*}

^aShanghai Institute of Ceramics, 1295 Dingxi Road, Shanghai 200050, China

^bDepartment of Chemistry, Northwestern University, 2145 Sheridan Road, Evanston, IL 60208-3113, USA

Received 27 August 2007; received in revised form 4 January 2008; accepted 6 January 2008

Available online 19 January 2008

Abstract

The compound $\text{Na}_5\text{Li}_3\text{Ti}_2\text{S}_8$ has been synthesized by the reaction of Ti with a Na/Li/S flux at 723 K. $\text{Na}_5\text{Li}_3\text{Ti}_2\text{S}_8$ crystallizes in a new structure type with four formula units in space group $C2/c$ of the monoclinic system. The structure contains three crystallographically independent Na^+ cations and two crystallographically independent Li^+ cations. $\text{Na}_5\text{Li}_3\text{Ti}_2\text{S}_8$ possesses a channel structure that features two-dimensional $[\text{LiTiS}_4]^{3-}$ layers built from $\text{Li}(1)\text{S}_4$ and TiS_4 tetrahedra. The layers, which are stacked along c , comprise eight-membered rings and sixteen-membered rings. $\text{Na}(3)^+$ cations are located between the eight-membered rings and $\text{Na}(1)^+$, $\text{Na}(2)^+$, and $\text{Li}(2)^+$ cations are located between the sixteen-membered rings. These cations are each octahedrally coordinated by six S^{2-} anions. The ionic conductivity σ_T of $\text{Na}_5\text{Li}_3\text{Ti}_2\text{S}_8$ ranges from 8.8×10^{-6} S/cm at 303 K to 3.8×10^{-4} S/cm at 483 K. The activation energy E_a is 0.40 eV.

© 2008 Elsevier Inc. All rights reserved.

Keywords: Sodium lithium titanium sulfide; Synthesis; X-ray structure; Channel structure; Ionic conductivity

1. Introduction

Lithium-ion secondary batteries are used as a power source for a wide range of portable electronic devices. These batteries would benefit from incorporation of a nonflammable solid electrolyte, a fast-ion conductor. Because chalcogen anions (Q^{2-}) are more polarizable than the oxygen anion (O^{2-}) chalcogenides often have much better conduction properties than the related oxides. For example, the room-temperature ionic conductivity of $60\text{Li}_2\text{S} \cdot 40\text{SiS}_2$ is 10^{-3} S/cm whereas that of $60\text{Li}_2\text{O} \cdot 40\text{SiO}_2$ is about 10^{-6} S/cm [1–3]. Among chalcogenide systems studied as fast-ion conductors have been AgPS_3 [4,5], $\text{Ag}_2\text{S} \cdot \text{GeS}_2$ [6,7], Ag_7NbS_6 [8], Li_2GeS_3 [9], Li_4GeS_4 [9], $\text{Li}_2\text{ZnGeS}_4$ [9], $\text{Li}_{4-2x}\text{Zn}_x\text{GeS}_4$ [9], and $\text{Ag}_{0.39}\text{TiS}_2$, [10].

Many compounds of the type $A/M/M'/Q$ (A = alkali metal; M = Li, Ag, Cu; M' = Ti, Zr, Nb, Ta) possess open-framework or channel structures [11–18]. For only a few were physical properties measured [14,17]. Here we

describe the synthesis, crystal structure, and conductivity of a new compound in this series, namely $\text{Na}_5\text{Li}_3\text{Ti}_2\text{S}_8$.

2. Experimental section

2.1. Synthesis of $\text{Na}_5\text{Li}_3\text{Ti}_2\text{S}_8$

The following reagents were used as obtained: Li_2S (Aldrich, 98%), Na_2S (Alfa Aesar, 98%), Ti (Aldrich, 99.7%), and S (Alfa Aesar, 99.5%). The compound $\text{Na}_5\text{Li}_3\text{Ti}_2\text{S}_8$ was synthesized from the reaction of 1.0 mmol Ti, 3.0 mmol S, 1.0 mmol Li_2S , and 2.0 mmol Na_2S . The reaction mixture was loaded into a fused-silica tube under an Ar atmosphere in a glove box. The tube was sealed under a 10^{-4} Torr atmosphere and then placed in a computer-controlled furnace. The sample was heated to 723 K in 24 h, kept at 723 K for 72 h, cooled at 3.5 K/h to 373 K, and then the furnace was turned off. The reaction mixture was washed with *N,N*-dimethylformamide and then dried with acetone. Red crystals of $\text{Na}_5\text{Li}_3\text{Ti}_2\text{S}_8$, suitable for a single-crystal X-ray diffraction study, were obtained in approximately 85% yield (based on Ti). The other material in the tube was a powder of unknown

*Corresponding author. Fax: +1 847 491 2976.

E-mail address: ibers@chem.northwestern.edu (J.A. Ibers).

composition. Examination of selected crystals with an EDX-equipped Hitachi S-3500 SEM led to results consistent with the stated composition. The compound is moderately stable in air.

2.2. Structure determination

Single-crystal X-ray diffraction data were collected with the use of graphite-monochromatized MoK α radiation ($\lambda = 0.71073$ Å) at 153 K on a Bruker Smart-1000 CCD diffractometer [19]. The crystal-to-detector distance was 5.023 cm. Crystal decay was monitored by recollecting 50 initial frames at the end of the data collection. Data were collected by a scan of 0.3° in ω in four groups of 606 frames at φ settings of 0° , 90° , 180° , and 270° . The exposure time was 15 s/frame. The collection of the intensity data was carried out with the program SMART [19]. Cell refinement and data reduction were carried out with the use of the program SAINT [19] and face-indexed absorption corrections were performed numerically with the use of the program XPREP [20]. Then the program SADABS [19] was employed to make incident beam and decay corrections.

The structure was solved with the direct methods program SHELXS and refined with the full-matrix least-squares program SHELXL [20]. The final refinement included anisotropic displacement parameters. The program TIDY [21] was then employed to standardize the atomic coordinates. Additional experimental details are shown in Table 1 and in the Supporting information. Table 2 presents selected metrical information.

2.3. AC impedance measurement

The ionic conductivity of Na₅Li₃Ti₂S₈ was measured in a dry argon atmosphere by means of a complex impedance determination on an impedance analyzer (Chenhua 660B)

Table 1
Crystal data and structure refinement for Na₅Li₃Ti₂S₈

Formula mass	488.05
Space group	C2/c
<i>a</i> (Å)	17.578(1)
<i>b</i> (Å)	9.6404(5)
<i>c</i> (Å)	12.0796(7)
β (deg)	133.4047(7)
<i>V</i> (Å ³)	1487.2(1)
<i>Z</i>	4
<i>T</i> (K)	153(2)
λ (Å)	0.71073
ρ_c (g/cm ³)	2.180
μ (cm ⁻¹)	23.03
<i>R</i> (<i>F</i>) ^a	0.0259
<i>R</i> _w (<i>F</i> _o) ^b	0.0780

^a $R(F) = \sum ||F_o| - |F_c|| / |F_o|$ for $F_o^2 > 2\sigma(F_o^2)$.

^b $R_w(F_o^2) = \{ \sum [w(F_o^2 - F_c^2)^2] / \sum w F_o^4 \}^{1/2}$; $w^{-1} = \sigma^2(F_o^2) + (0.04 \times F_o^2)^2$ for $F_o^2 \geq 0$ and $w^{-1} = \sigma^2(F_o^2)$ for $F_o^2 < 0$.

Table 2
Selected distances (Å) in Na₅Li₃Ti₂S₈

Na(1)–S1	2.8189(9)	Na(3)–S3 × 2	2.7504(5)
Na(1)–S4	2.8815(9)	Na(3)–S4 × 2	2.9817(9)
Na(1)–S2	2.9781(8)	Li(1)–S1	2.399(3)
Na(1)–S3	2.9979(8)	Li(1)–S2	2.430(3)
Na(1)–S4	3.0812(9)	Li(1)–S3	2.445(3)
Na(1)–S4	3.3323(9)	Li(1)–S4	2.499(3)
Na(2)–S1	2.7823(8)	Li(2)–S1 × 2	2.8745(4)
Na(2)–S2	2.9470(8)	Li(2)–S2 × 2	2.9028(4)
Na(2)–S2	2.9998(8)	Li(2)–S3 × 2	2.4937(4)
Na(2)–S2	3.1762(8)	Ti–S1	2.2405(5)
Na(2)–S3	2.8741(8)	Ti–S3	2.2647(5)
Na(2)–S4	2.8384(8)	Ti–S2	2.2775(5)
Na(3)–S1 × 2	2.9063(8)	Ti–S4	2.2788(5)

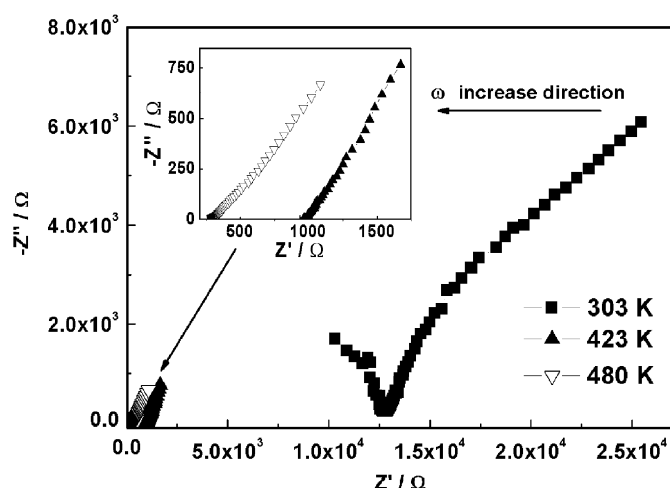


Fig. 1. Complex impedance plots for the sample of Na₅Li₃Ti₂S₈. The frequency increases for each point from right to left starting at 0.1 Hz and ending at 0.1 MHz.

in the frequency range 0.1 Hz–0.1 MHz over the temperature range 303–483 K. About 0.3 g of crystals were ground into a fine powder in a glove box. This powder was converted to a pellet about 10 mm in diameter by 1.2 mm high by cold pressing at 10 MPa. Indium plates (~0.03 mm thick) were attached to both sides of the pelletized sample to serve as current collectors.

The conductivities of Na₅Li₃Ti₂S₈ were examined from the Nyquist plots, as shown in Fig. 1 [22]. The total resistance was obtained from the intersection of the semicircle with the real (*Z'*) axis at the lower frequency side in each of the complex impedance plots. At 303 K an incomplete semicircle in the high-frequency range and a spike in the low-frequency range were observed. The semicircle can be interpreted as a parallel combination of a resistance and the spike that was caused by an electrode contribution [23,24]. Such spikes disappeared with increasing temperature. The resistances were converted to dc conductivities from the sample thickness and electrode area of the pelletized sample.

3. Results

3.1. Synthesis

The new compound $\text{Na}_5\text{Li}_3\text{Ti}_2\text{S}_8$ has been synthesized in greater than 85% yield from the reaction of Ti with a Na/Li/S flux at 723 K.

3.2. Crystal structure

There are no metal–metal or S–S bonds in the structure. Accordingly, the formal oxidation states of Na, Li, Ti, and

S may be assigned as 1+, 1+, 4+, and 2–, respectively. $\text{Na}_5\text{Li}_3\text{Ti}_2\text{S}_8$ crystallizes in a new structure type with four formula units in space group $C2/c$ of the monoclinic system. The crystal structure is illustrated in Fig. 2 and as a polyhedral representation in Fig. 3. In the structure there are three crystallographically unique Na^+ cations and two unique Li^+ cations. Given our somewhat arbitrary choice of describing the $\text{Li}(1)^+$ cations as belonging to the framework and the $\text{Li}(2)^+$ cations as being isolated, the structure comprises ${}^2_\infty[\text{Li}(1)\text{TiS}_4^-]$ layers perpendicular to c (Fig. 2). The layers are separated by Na^+ and $\text{Li}(2)^+$ cations. A ${}^2_\infty[\text{Li}(1)\text{TiS}_4^-]$ layer consists of $\text{Li}(1)\text{S}_4$ and TiS_4

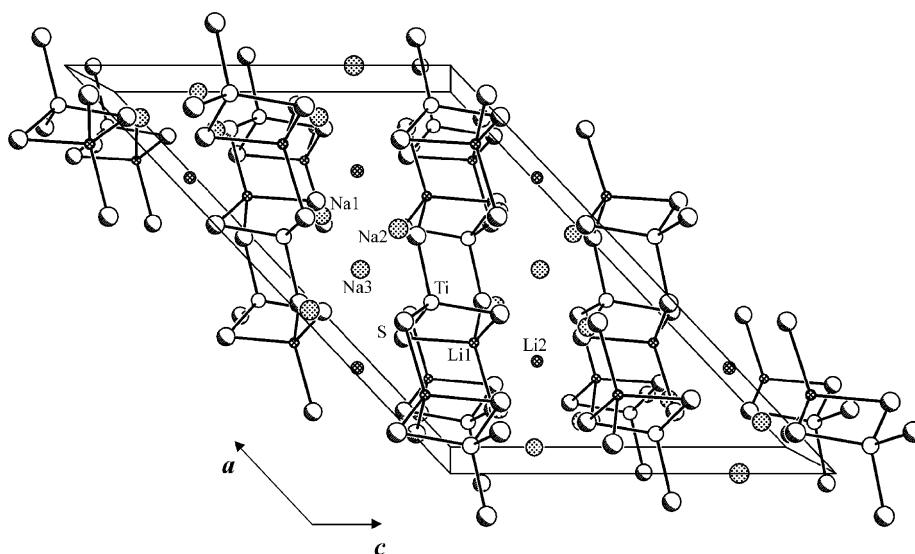


Fig. 2. The structure of $\text{Na}_5\text{Li}_3\text{Ti}_2\text{S}_8$ viewed down [010]. For the sake of clarity, the Na–S and Li(2)–S interactions have been omitted.

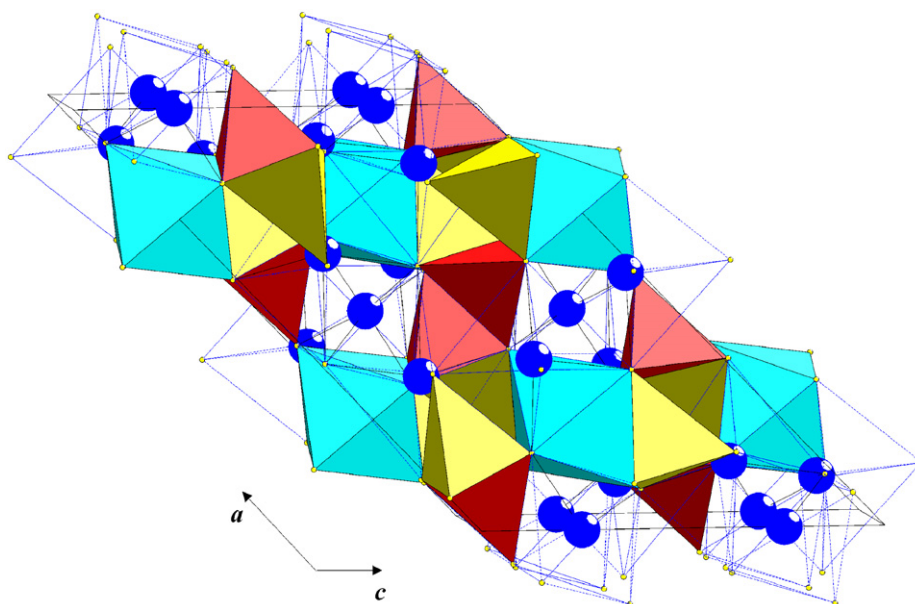


Fig. 3. Polyhedral representation of the structure of $\text{Na}_5\text{Li}_3\text{Ti}_2\text{S}_8$ in the same orientation as Fig. 1. $\text{Li}(1)\text{S}_4$ tetrahedra are yellow, $\text{Li}(2)\text{S}_6$ octahedra are olive green, TiS_4 tetrahedra are red, and all the NaS_6 octahedra are blue and open.

tetrahedra. Each $\text{Li}(1)\text{S}_4$ tetrahedron links to four TiS_4 tetrahedra by sharing two vertices (S1, S2) and one edge (S3, S4), and each TiS_4 tetrahedron connects to $\text{Li}(1)\text{S}_4$ tetrahedra by the same linkages, as shown in Fig. 4. A layer comprises eight-membered rings and sixteen-membered rings (Fig. 4). $\text{Na}(3)^+$ cations are located between the eight-member rings and $\text{Na}(1)^+$, $\text{Na}(2)^+$, and $\text{Li}(2)^+$ cations are located between the sixteen-membered rings, as shown in Fig. 4. These cations are octahedrally coordinated by six S^{2-} anions. Of course, this channel structure is not closed packed; there is room for movement of these cations.

Selected metrical data for the $\text{Na}_5\text{Li}_3\text{Ti}_2\text{S}_8$ structure are listed in Table 2. In $\text{Na}_5\text{Li}_3\text{Ti}_2\text{S}_8$, the Na–S distances of 2.7504(5)–3.3323(9) Å are in the range of 2.857(4)–3.201(4) Å found in $\text{Na}_2\text{Cu}_2\text{ZrS}_4$ [11]. The Li–S distances in the $\text{Li}(1)\text{S}_4$ tetrahedron (2.399(3)–2.499(3) Å) are similar to those of 2.381(8)–2.505(8) Å in $\text{Rb}_2\text{LiNbS}_4$ [18], and those in the $\text{Li}(2)\text{S}_6$ octahedron (2.4937(4)–2.9028(4) Å) are in the range of those of 2.55(5)–3.10(3) Å in the LiS_6 octahedron of Li_4GeS_4 [25]. The Ti–S distances of 2.2405(5)–2.2788(5) Å are consistent with that of 2.2775(8) Å in $\text{Rb}_2\text{Cu}_2\text{TiS}_4$ [17].

3.3. Ionic conductivity

Fig. 5 and Table 3 show the temperature dependence of the conductivity for the sample of $\text{Na}_5\text{Li}_3\text{Ti}_2\text{S}_8$. The plot of $\log(\sigma)$ against $10^3/T$ indicates that the conductivities in the temperature range 303–483 K follow the Arrhenius equation $\sigma = \sigma_0 \exp(-E_a/kT)$, where σ is the total conductivity of the electrolyte, σ_0 is the pre-exponential parameter, k is the Boltzmann constant, T is the Kelvin temperature, and E_a is the activation energy. From the crystal structure of $\text{Na}_5\text{Li}_3\text{Ti}_2\text{S}_8$, the interaction between two neighboring Ti centers can be neglected because the shortest Ti...Ti distance is 5.162 Å. Thus, the electronic conductivity should be considerably smaller than the ionic conductivity. This is consistent with the results shown in Fig. 5. Accordingly, the activation energy for ionic conductivity E_a is calculated to be 0.40 eV from the above equation. The conductivities of the sample are 8.8×10^{-6} S/cm at 303 K and 2.3×10^{-4} S/cm at 453 K, higher than those of typical sulfide electrolytes (Table 4).

In the present structure the Li–S bonds in the $\text{Li}(1)\text{S}_4$ tetrahedron are shorter, and presumably stronger, than those in the $\text{Li}(2)\text{S}_6$ octahedron. In this channel structure

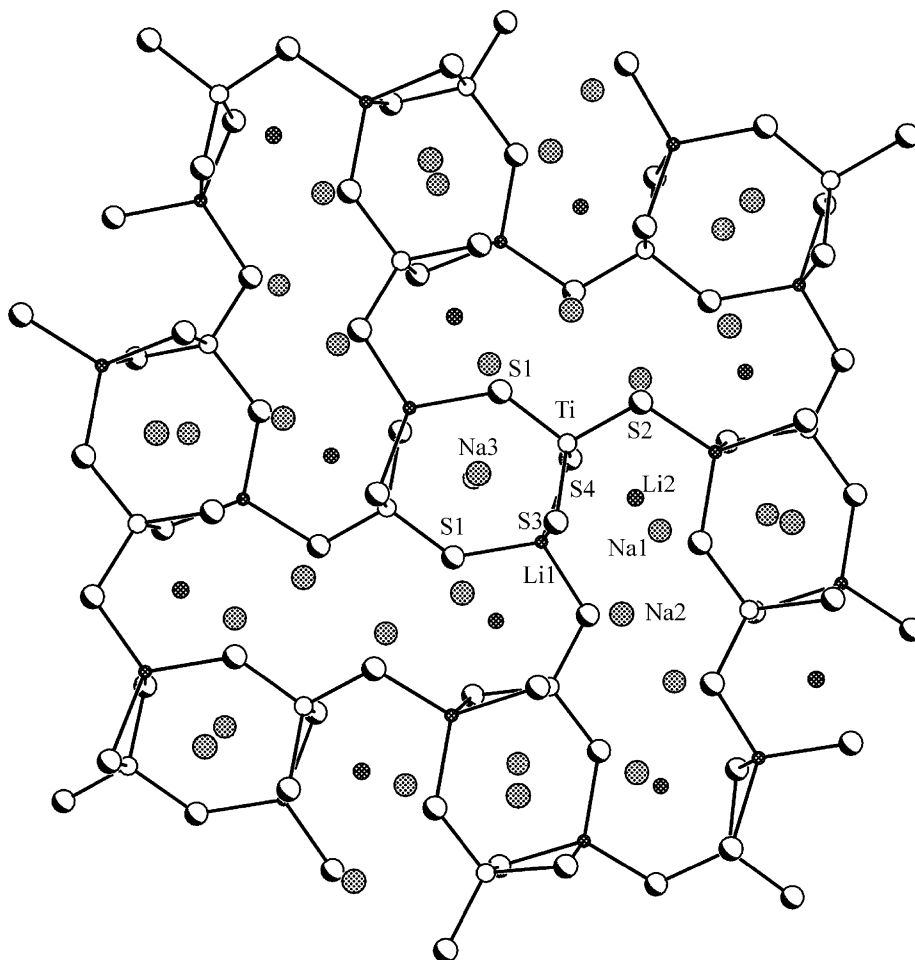


Fig. 4. Two-dimensional $[\text{Li}(1)\text{TiS}_4]_{\infty}^{2-}$ layer of $\text{Na}_5\text{Li}_3\text{Ti}_2\text{S}_8$ viewed down c .

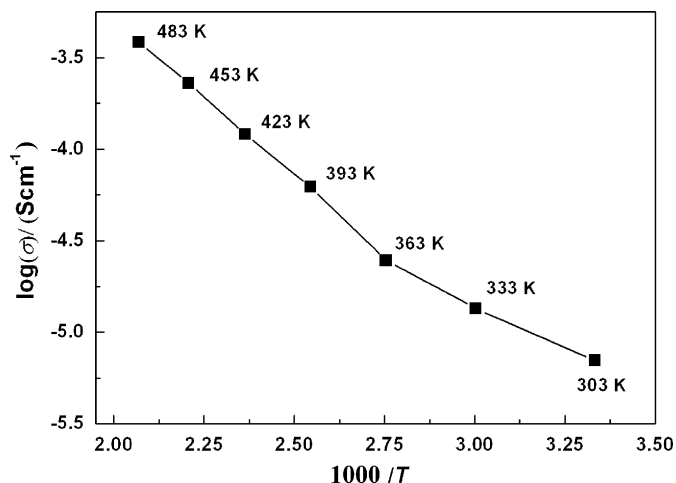


Fig. 5. Reciprocal temperature dependence of the logarithmic conductivity for the sample of $\text{Na}_5\text{Li}_3\text{Ti}_2\text{S}_8$.

Table 3
Conductivity (σ) of $\text{Na}_5\text{Li}_3\text{Ti}_2\text{S}_8$ as a function of temperature (T)

σ (S/cm)	T (K)
8.8×10^{-6}	303
1.4×10^{-5}	333
1.9×10^{-5}	363
6.2×10^{-5}	393
1.2×10^{-4}	423
2.3×10^{-4}	453
3.8×10^{-4}	483

Table 4
Ionic conductivities of selected compounds

Compound	Ionic conductivity (S/cm, 298 K)	Activation energy (eV)	Reference
$\text{Na}_5\text{Li}_3\text{Ti}_2\text{S}_8$	8.8×10^{-6}	0.40	This work
$\text{Na}_{1+x}\text{Zr}_2\text{Si}_x\text{P}_{3-x}\text{O}_{12}$	$\approx 10^{-3}$		[26]
Li_2SiO_3	6.0×10^{-8}		[27]
Li_2SiS_3	2.0×10^{-6}	0.49	[28]
Li_3PS_4	3×10^{-7}	0.46	[29]
$\text{LiTi}_2(\text{PO}_4)_3$ (NASICON-type)	$\approx 10^{-6}$ – 10^{-8}		[30]
$\text{Li}_3\text{Fe}_2(\text{PO}_4)_3$	$\approx 10^{-8}$		[31]

we would expect the $\text{Li}(2)^+$ cations to be freer to move. Similarly, the Na^+ cations atoms are expected to be movable owing to the surrounding available space. Some typical values of Na^+ and Li^+ ionic conductivities are given in Table 4. The change in slope in Fig. 5 may reflect competition between $\text{Li}(2)^+$ transport and Na^+ transport.

Supporting information

Crystallographic data in CIF format for $\text{Na}_5\text{Li}_3\text{Ti}_2\text{S}_8$ have been deposited with FIZ Karlsruhe as CSD number

391258. The data may be obtained free of charge by contacting FIZ Karlsruhe at +49 7247 808 666 (fax) or crysdta@fiz-karlsruhe.de (email).

Acknowledgments

This research was supported by the Science and Technology Commission of Shanghai Municipality (Grant no. 05JC14080). Use was made of the Central Facilities supported by the MRSEC program of the National Science Foundation (DMR05-20513) at the Materials Research Center of Northwestern University.

References

- [1] A. Pradel, M. Ribes, *Solid State Ionics* 18–19 (1986) 351–355.
- [2] A. Hayashi, R. Araki, R. Komiya, K. Tadanaga, M. Tatsumisago, T. Minami, *Solid State Ionics* 113–115 (1998) 733–738.
- [3] J.H. Kennedy, *Mater. Chem. Phys.* 23 (1989) 29–50.
- [4] Y. Kawamoto, M. Nishida, *J. Non-Cryst. Solids* 20 (1976) 393–404.
- [5] Z. Zhang, J.H. Kennedy, *J. Electrochem. Soc.* 140 (1993) 2384–2390.
- [6] J.L. Souquet, E. Robinel, *Solid State Ionics* 3/4 (1981) 317–321.
- [7] F. Salam, S.S. Soulayman, J.C. Giuntini, J.V. Zanchetta, *Solid State Ionics* 83 (1996) 235–243.
- [8] H. Wada, *J. Alloys Compd.* 178 (1992) 315–323.
- [9] R. Kanno, T. Hata, Y. Kawamoto, M. Irie, *Solid State Ionics* 130 (2000) 97–104.
- [10] A.G. Gerards, H. Roede, R.J. Haange, B.A. Boukamp, G.A. Wieggers, *Synth. Met.* 10 (1984) 51–66.
- [11] M.F. Mansuetto, J.A. Ibers, *J. Solid State Chem.* 117 (1995) 30–33.
- [12] M.F. Mansuetto, J.A. Cody, S. Chien, J.A. Ibers, *Chem. Mater.* 7 (1995) 894–898.
- [13] M.A. Pell, J.A. Ibers, *J. Am. Chem. Soc.* 117 (1995) 6284–6286.
- [14] M.F. Mansuetto, P.M. Keane, J.A. Ibers, *J. Solid State Chem.* 101 (1992) 257–264.
- [15] M.F. Mansuetto, P.M. Keane, J.A. Ibers, *J. Solid State Chem.* 105 (1993) 580–587.
- [16] F.Q. Huang, K. Mitchell, J.A. Ibers, *Inorg. Chem.* 40 (2001) 5123–5126.
- [17] F.Q. Huang, J.A. Ibers, *Inorg. Chem.* 40 (2001) 2602–2607.
- [18] F.Q. Huang, B. Deng, J.A. Ibers, *J. Solid State Chem.* 178 (2005) 194–199.
- [19] Bruker, SMART Version 5.054 Data Collection and SAINT-Plus Version 6.45a Data Processing Software for the SMART System, Bruker Analytical X-ray Instruments, Inc., Madison, WI, USA, 2003.
- [20] G.M. Sheldrick, SHELXTL Version 6.14, Bruker Analytical X-ray Instruments, Inc., Madison, WI, USA, 2003.
- [21] L.M. Gelato, E. Parthé, *J. Appl. Crystallogr.* 20 (1987) 139–143.
- [22] E. Barsoukov, J.R. Macdonald (Eds.), *Impedance Spectroscopy*. 2nd ed., Wiley-Interscience, Hoboken, NJ, 2005.
- [23] J.R. Macdonald, *Impedance Spectroscopy: Emphasizing Solid Materials and Systems*, John Wiley & Sons, Inc., New York, 1987.
- [24] P. Fragnaud, D.M. Schleich, *Sensors Actuators A* 51 (1995) 21–23.
- [25] Y. Matsushita, M.G. Kanatzidis, *Z. Naturforsch. B: Chem. Sci.* 53 (1998) 23–30.
- [26] D. Zhu, F. Luo, Z. Xie, W. Zhou, *Rare Metals* 25 (2006) 39–42.
- [27] I.D. Raistrick, C. Ho, R.A. Huggins, *J. Electrochem. Soc.* 123 (1976) 1469–1476.
- [28] B.T. Ahn, R.A. Huggins, *Mater. Res. Bull.* 24 (1989) 889–897.
- [29] M. Tachez, J.-P. Malugani, R. Mercier, G. Robert, *Solid State Ionics* 14 (1984) 181–185.
- [30] N. Kosova, E. Devyatkina, *J. Mater. Sci.* 39 (2004) 5031–5036.
- [31] A.K. Ivanov-Schitz, A.V. Nistuk, N.G. Chaban, *Solid State Ionics* 139 (2001) 153–157.